

Studies of the photoionization cross section of the 2π level of nitric oxide

Maile E. Smith, R. R. Lucchese,^{a)} and V. McKoy

Arthur Amos Noyes Laboratory of Chemical Physics,^{b)} California Institute of Technology, Pasadena, California 91125

(Received 20 October 1982; accepted 30 November 1982)

We present photoionization cross sections and asymmetry parameters for the 2π level of nitric oxide which are obtained from the direct solution of the $e + \text{NO}^+$ collisional equations at the static-exchange level. These cross sections differ significantly from those obtained previously using a moment theory approach [J. J. Delaney, I. H. Hillier, and V. R. Saunders, *J. Phys. B* **15**, 1477 (1982)]. The calculated cross sections show a broad nonresonant feature at a photon energy of 29 eV which is not as pronounced as observed experimentally. The σ shape resonance in our cross section occurs at 14 eV which is about 5 eV below the feature in the measured cross sections attributed to this shape resonance. The probable role of autoionization and vibrational averaging on these cross sections is also discussed.

INTRODUCTION

Theoretical studies of molecular photoionization, which yield cross sections and photoelectron angular distributions, can provide an important probe of molecular electronic structure and dynamics.¹ With the tunable continuum provided by synchrotron radiation, the spectral variation of these cross sections and angular distributions can now be studied over a wide continuous range of incident photon energy. Such data have already shown that shape resonances play an important role in molecular photoionization.²

Recently, the photoionization cross sections of nitric oxide have been measured using both synchrotron radiation³ and the $(e, 2e)$ pseudophoton technique.⁴ The measured cross sections for photoionization out of the 2π level show two resonantlike features at photon energies of 19 and 29 eV with the feature at 29 eV being very broad. This partial cross section has also been studied recently by the Stieltjes–Tchebycheff moment theory (STMT) approach⁵ and by the continuum multiple-scattering method (MSM).⁶ In this paper, we present photoionization cross sections and asymmetry parameters for the 2π level of NO which are obtained from the direct solution of the $e + \text{NO}^+$ collisional equations at the static-exchange level. These cross sections differ significantly from those obtained by the STMT approach; in particular, the nonresonant $2\pi - k\pi$ and $2\pi - k\delta$ contributions to this partial cross section do not show the sharp structure seen in the STMT results⁵ at photon energies between 13 and 17 eV. Our calculated cross sections also suggest that the broad feature at a photon energy of 29 eV is nonresonant and arises from the energy dependence of the $2\pi - k\pi$ and $2\pi - k\delta$ dipole matrix elements. However, this feature is not as pronounced in the calculated cross sections as is observed experimentally and moreover, our cross sections are smaller than the measured cross sections in this region. At the equilibrium geometry our calculated cross sections show a σ shape resonance around 14 eV which is about

5 eV below the feature in the measured cross sections which has been attributed to this shape resonance.^{3,6} The implication and a probable explanation of this difference are discussed.

THEORY AND CALCULATIONAL DETAILS

The rotationally unresolved, fixed-nuclei photoionization cross section is given by

$$\sigma_{i,f}(R) = \frac{4\pi^2\omega}{3} |\langle \Psi_i(\mathbf{r}, R) | \mu | \Psi_f(\mathbf{r}, R) \rangle|^2, \quad (1)$$

where μ is the dipole moment operator and ω the photon frequency. In Eq. (1), $\Psi_i(\mathbf{r}, R)$ is the initial state of the molecule and $\Psi_f(\mathbf{r}, R)$ the final ionized state. For $\Psi_i(\mathbf{r}, R)$ we use the ground state SCF wave function and for the $(N-1)$ bound electrons of $\Psi_i(\mathbf{r}, R)$ we use the ground state SCF orbitals, i.e., the frozen-core approximation. The continuum orbital in $\Psi_f(\mathbf{r}, R)$ for the ejected electron is a solution of the one-particle Schrödinger equation with the static-exchange potential V_{N-1} of the ion. The continuum orbital satisfies the equation

$$\left[-\frac{1}{2} \nabla^2 + V_{N-1}(\mathbf{r}, R) - \frac{k^2}{2} \right] \psi_{\mathbf{k}}(\mathbf{r}, R) = 0, \quad (2)$$

where $k^2/2$ is the kinetic energy of the ejected electron.

The partial wave component of $\psi_{\mathbf{k}}, \psi_{klm}$ then satisfies the Lippmann–Schwinger equation

$$\psi_{klm}^{(-)} = \phi_{klm} + G_C^{(-)} U \psi_{klm}^{(-)}, \quad (3)$$

where $G_C^{(-)}$ is the Coulomb Green's function with incoming-wave boundary conditions, ϕ_{klm} the regular Coulomb function, and $U = 2V$ where V is the potential of the molecular ion with the Coulomb component removed. We have recently developed an iterative approach to the solution of the Lippmann–Schwinger equation which is based on the Schwinger variational principle.⁷ Applications^{8,9} have shown that the method is a very effective approach to electron-molecular ion collisions at energies where partial wave coupling due to nonspherical potentials and exchange effects are important. Details have been discussed elsewhere.⁷ In this approach, we first solve the Lippmann–Schwinger equation by assuming an approximate separable form for

^{a)}Present address: Bell Laboratories, Murray Hill, New Jersey 07974.

^{b)}Contribution No. 6746.

the scattering potential U , i. e.,

$$U(\mathbf{r}, \mathbf{r}') \approx U^S(\mathbf{r}, \mathbf{r}') = \sum_{i,j} \langle \mathbf{r} | U | \alpha_i \rangle (U^{-1})_{ij} \langle \alpha_j | U | \mathbf{r}' \rangle, \quad (4)$$

where the matrix $(U^{-1})_{ij}$ is the inverse of the matrix $U_{ij} = \langle \alpha_i | U | \alpha_j \rangle$. The functions α_i are initially chosen to be discrete basis functions such as Cartesian or spherical Gaussian functions. The solution of Eq. (3) for the potential U^S is simply

$$\psi_{klm}^{(0)}(\mathbf{r}) = \phi_{klm} + \sum_{i,j} \langle \mathbf{r} | G_C U | \alpha_i \rangle (D^{-1})_{ij} \langle \alpha_j | U | \phi_{klm} \rangle, \quad (5)$$

where the matrix $(D^{-1})_{ij}$ is the inverse of the matrix

$$D_{ij} = \langle \alpha_i | U - U G_C U | \alpha_j \rangle. \quad (6)$$

The solutions $\psi_{klm}^{(0)}$ provide the initial estimates of the photoionization cross sections which are, at this stage, variationally stable. However, these functions $\psi_{klm}^{(0)}$ are solutions of the Lippmann-Schwinger equation for separable potential U^S , and not for the actual scattering potential U . To obtain more accurate and, if necessary, converged solutions of Eq. (3) we have developed a method to iteratively improve the solutions of Eq. (5) $\psi_{klm}^{(0)}$. The procedure contains criteria which allow one to determine when the exact solutions of the scattering problem have been obtained.¹⁰ Such solutions provide increasingly accurate estimates of both the photoionization cross section and photoelectron asymmetry parameters.

We have used this procedure to study the photoionization out of the 2π level of NO at the static-exchange frozen-core approximation.⁸ The target wave function was constructed from the same $[5s, 3p, 1d]$ contracted Cartesian Gaussian basis set as used in the STMT calculations of Ref. 5. The SCF energy of NO at the ground state equilibrium separation of 2.173 a. u. in this basis is -129.269 a. u. All matrix elements are evaluated by a single-center expansion and the radial integrals are computed by Simpson's rule.¹¹ To assure convergence we truncated these expansions as follows:

(i) Maximum partial wave retained in the expansion of the scattering function $= l_{\max} = 20$. (ii) Maximum partial wave retained in the expansion of the scattering function in the exchange matrix elements $= l_{\max}^{\text{ex}} = 20$. (iii) Maximum partial wave retained in the expansion of $1/r_{12}$ in the direct potential (not including the nuclear terms) $= \lambda_{\max} = 20$. We always include $2\lambda_{\max}$ terms in the expansion of the nuclear potential. (iv) Maximum partial wave in the expansion of the i th occupied orbital in the exchange matrix elements $= l_i^{\text{ex}}$. These values of l_i^{ex} are chosen so that the orbitals are normalized to better than 0.99 and range from 20 for the 1σ orbital to 10 for the 1π orbital.

This truncation of the partial wave expansions should assure convergence of the calculated matrix elements and cross sections. For example, reduction of the expansion parameters to $l_{\max} = 16$, $\lambda_{\max} = 16$, $l_{\max}^{\text{ex}} = 16$, $l_i^{\text{ex}}(1\sigma) = 16$, and $l_i^{\text{ex}}(1\pi) = 6$ leads to changes of about 3% in the eigenphase sum and less than 0.5 eV in the position of the resonance. In the nonresonant regions this error was considerably smaller. All radial integrands were expanded on a grid of 800 points extending out to

64 a. u. The smallest step size in this grid was 0.01 a. u., which was used out to 2 a. u., and the largest step size was 0.16 a. u.

The photoionization cross sections reported here were calculated with continuum wave functions obtained after one or two steps in the iterative procedure.¹⁰ In general the cross sections obtained with the uniterated scattering functions, i. e., the $\psi_{klm}^{(0)}$ of Eq. (5) were accurate to within 2% in the nonresonant regions and to within 15% in the resonance region. The starting basis sets for these calculations contained a total of 18 Gaussian functions for the $k\sigma$ and $k\pi$ channels and 17 for the $k\delta$ channel.

RESULTS AND DISCUSSION

Figure 1 shows our calculated results for the $2\pi \rightarrow k\sigma$, $2\pi \rightarrow k\pi$, and $2\pi \rightarrow k\delta$ components of the fixed-nuclei ($R = 2.173$ a. u.) photoionization cross sections for the 2π level of NO. The photon energy scale assumes an ionization potential of 9.3 eV. The $2\pi \rightarrow k\sigma$ component of the cross section is very clearly enhanced by a shape resonance centered at about 5 eV of photoelectron kinetic energy. The calculated eigenphases show a very strong mixing of the p and f waves in this region. These results also show that the $2\pi \rightarrow k\pi$ and $k\delta$ cross sections are nonshape resonant. Their enhancement around a photon energy of 24 eV is due to the general energy dependence of the dipole matrix elements for the 2π valence level. The $2\pi \rightarrow k\pi$ and $k\delta$ components will hence be insensitive to changes in the internuclear distance.

Figure 2 shows the $2\pi \rightarrow k\sigma$, $k\pi$, and $k\delta$ photoionization cross sections of Delaney *et al.*⁵ using a six-point Tchebycheff imaging procedure.¹² A comparison of our results in Fig. 1 with those of Fig. 2 show that our $2\pi \rightarrow k\pi$ and $k\delta$ cross sections do not show the sharp structure seen between 13 and 17 eV in the results of the Tchebycheff imaging procedure.⁵ Moreover, the general shape of the $k\pi$ and $k\delta$ cross sections of the imaging procedure⁵ is substantially different from those of the pres-

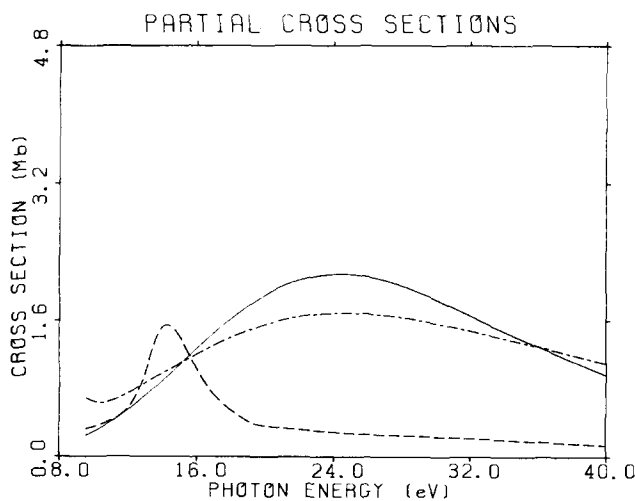


FIG. 1. Components of the calculated photoionization cross section for the 2π level of NO in the present work: (---) $2\pi \rightarrow k\sigma$, (—) $2\pi \rightarrow k\pi$, (-·-·) $2\pi \rightarrow k\delta$.

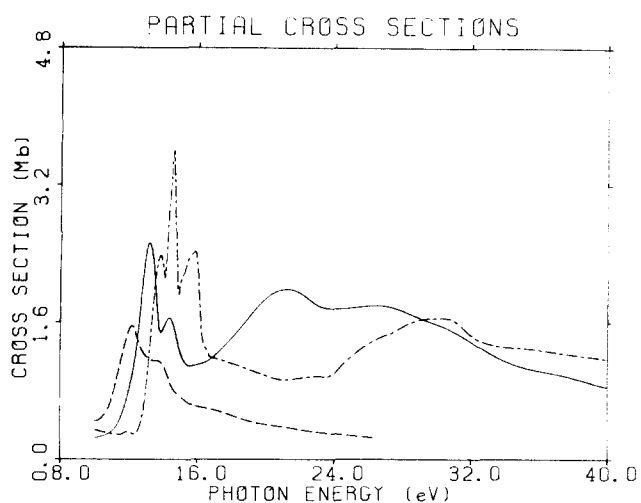


FIG. 2. Components of the calculated photoionization cross section for the 2π level of NO, from Ref. 5, using the Tchebycheff imaging technique: (---) $2\pi \rightarrow k\sigma$, (—) $2\pi \rightarrow k\pi$, (- - -) $2\pi \rightarrow k\delta$.

ent calculations. We note that these calculations are both done at the static-exchange level using the same molecular ion potential. These results suggest that the sharp structure in these $k\pi$ and $k\delta$ cross sections⁵ is spurious and may, in fact, be due to the inclusion of insufficient or unconverged moments of the oscillator strength distribution in these calculations.¹³

In Fig. 3 we compare our calculated 2π photoionization cross sections with the experimental results obtained by synchrotron radiation³ and $(e, 2e)$ ⁴ measurements. Figure 3 also includes the cross sections obtained by the Tchebycheff imaging procedure⁵ and the continuum multiple scattering method.⁶ The multiple scattering cross sections are vibrationally averaged while the other calculated results are for the nuclei fixed at $R = 2.173$ a. u.

The shape resonance feature is evident around 14 eV in our calculated cross section. The experimental data³ extends only down to photon energies of 16 eV and, moreover, shows a feature at around 18 eV which has been attributed to the shape-resonant σ continuum.^{3,6} The vibrationally averaged cross sections of the multiple scattering method do show a weak resonant feature around 19 eV. Our experience suggests that vibrational averaging of the fixed-nuclei cross sections for the $v=0$ level will not shift the resonant feature from its present position of 14 eV up to around 19 eV.¹⁴ As a quantitative check we calculated the $2\pi \rightarrow k\sigma$ fixed-nuclei cross sections at an internuclear distance of 2.003 a. u., the equilibrium value of the ion. As expected, the resonance feature was broadened and shifted to higher energy (~ 19 eV) but its peak value was essentially unchanged. Vibrational averaging of such cross sections will not move the position of the resonance peak significantly away from its value at the equilibrium internuclear distance of 2.173. Studies of the vibrationally resolved photoionization cross sections down to 12 eV of photon energy can help clarify the origin of these features.

The role of autoionizing states in this region should also be explored.

Our results show a very broad feature between 20 and 32 eV which is nonresonant and simply due to the dependence of the $2\pi \rightarrow k\pi$ and $k\delta$ dipole matrix elements on photon energy. The calculated cross sections do not adequately account for the broad resonancelike feature observed experimentally around 29 eV. Vibrational averaging is not expected to have any significant effect on these nonresonant cross sections and a numerical test carried out at $R = 2.003$ a. u. confirmed this. We also note that the cross sections obtained in this energy region by the Tchebycheff imaging technique⁵ lie well below the experimental values.³ Moreover, this feature is also not seen in the continuum multiple scattering results.⁶ These results suggest that the broad enhancement of the cross section around 28 eV could be due to unresolved bands of autoionizing lines converging to a higher ionic level. Vibrationally resolved studies in this region are clearly needed.

In Fig. 4 we compare our calculated photoelectron asymmetry parameters with the measured values. Although the results account for the rise of these parameters with energy, the calculated values are too high. Measurements of these parameters below 16 eV will be useful in view of the predicted behavior between 10 and 16 eV.

CONCLUSIONS

The results of these studies show that the broad feature in the measured cross section for the 2π level of NO around 29 eV is not due to a shape resonance and that the possible role of autoionization in this region should be examined. Our results also predict that the shape resonance due to the σ continuum is located around 14 eV which is about 5 eV below the feature in the measured cross sections which has been attributed

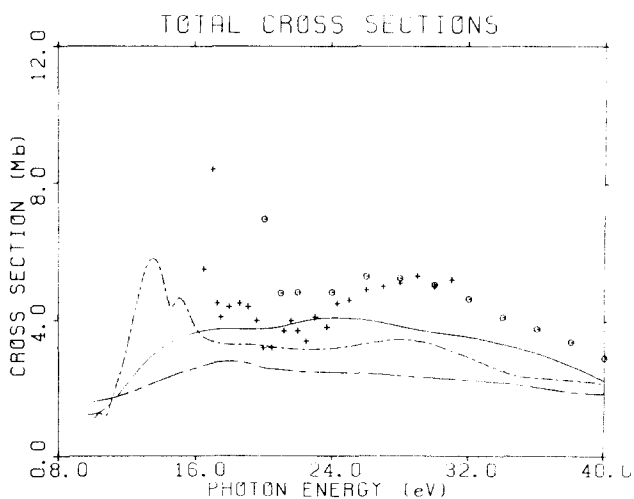


FIG. 3. A comparison of 2π photoionization cross sections in NO: (—) present fixed-nuclei ($R = 2.173$ a. u.) results, (---) Tchebycheff imaging results of Delaney *et al.* (Ref. 5), (- - -) vibrationally averaged results of the continuum multiple scattering model (Ref. 6), + synchrotron radiation measurements of Ref. 3, o $(e, 2e)$ measurements of Ref. 4.

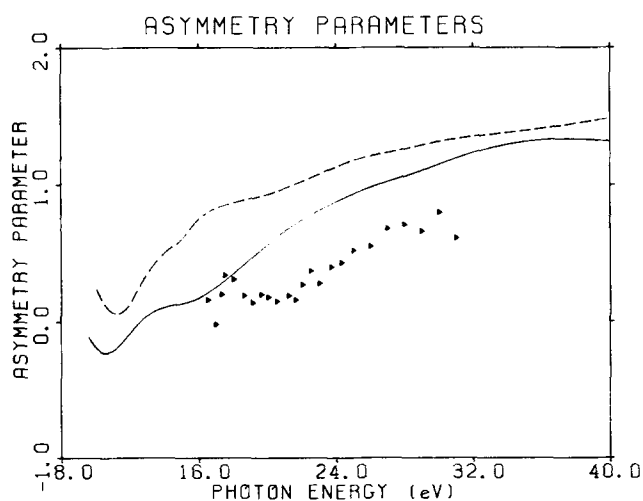


FIG. 4. A comparison of asymmetry parameters for 2π photoionization of NO: (—) present work using the fixed nuclei approximation, (---) vibrationally averaged results of the MSM (Ref. 6), \blacktriangle synchrotron radiation experiments of Ref. 3.

to a shape resonance.^{3,6} We have also shown that the sharp structure in the $k\pi$ and $k\delta$ components of the photoionization cross sections between 13 and 17 eV seen in the Tchebycheff imaging results⁵ is spurious. Extension of the present measurements to photon energies below 16 eV and vibrationally resolved studies of these photoionization cross sections are clearly needed.

ACKNOWLEDGMENTS

This material is based upon work supported by the National Science Foundation under Grant No. CHE80-

40870. One of us (M.E.S.) acknowledges support of a National Science Foundation Predoctoral Fellowship. The research reported in this paper made use of the Dreyfus-NSF Theoretical Chemistry Computer which was funded through grants from the Camille and Henry Dreyfus Foundation, the National Science Foundation (Grant No. CHE78-20235), and the Sloan Fund of the California Institute of Technology.

¹J. Berkowitz, *Photoabsorption, Photoionization, and Photoelectron Spectroscopy* (Academic, New York, 1979).

²See, for example, J. B. West, A. C. Parr, B. E. Cole, D. L. Ederer, R. Stockbauer, and J. L. Dehmer, *J. Phys. B* **13**, L105 (1980).

³S. Southworth, C. M. Truesdale, P. H. Korbin, D. W. Lindle, D. W. Brewer, and D. A. Shirley, *J. Chem. Phys.* **76**, 143 (1982).

⁴C. E. Brion and K. H. Tan, *J. Electron Spectrosc. Relat. Phenom.* **23**, 1 (1981).

⁵J. J. Delaney, I. H. Hillier, and V. R. Saunders, *J. Phys. B* **15**, 1477 (1982).

⁶S. Wallace, D. Dill, and J. L. Dehmer, *J. Chem. Phys.* **76**, 1217 (1982).

⁷R. R. Lucchese and V. McKoy, *Phys. Rev. A* **24**, 770 (1981).

⁸R. R. Lucchese, G. Raseev, and V. McKoy, *Phys. Rev. A* **25**, 2572 (1982).

⁹R. R. Lucchese and V. McKoy, *Phys. Rev. A* **26**, 1406 (1982).

¹⁰R. R. Lucchese, D. K. Watson, and V. McKoy, *Phys. Rev. A* **22**, 421 (1980).

¹¹R. R. Lucchese and V. McKoy, *Phys. Rev. A* **21**, 112 (1980).

¹²J. J. Delaney, V. R. Saunders, and I. H. Hillier, *J. Phys. B* **14**, 819 (1981).

¹³P. W. Langhoff, C. T. Corcoran, J. S. Sims, F. Weinhold, and R. M. Glover, *Phys. Rev. A* **14**, 1042 (1976).

¹⁴R. R. Lucchese and V. McKoy, *Phys. Rev. A* **26**, 1406 (1982).